

Precision machining and measurement of micro aspheric molds

H. Suzuki^{1,3}, T. Moriwaki², Y. Yamagata³, and T. Higuchi⁴

¹ Chubu University, Kasugai, Aichi, Japan

² Setsunan University, Neyagawa, Osaka, Japan

³ The Institute of Physical and Chemical Research, Wako, Saitama, Japan

⁴ University of Tokyo, Bunkyo, Tokyo, Japan

Abstract—Demands of micro aspheric optical components such as lenses and mirrors are increasing for installing to the digital devices such as DVD, Digital camera, mobile phone and virtual reality system. As the devices become to be more compact and complicated, the molds shapes of lens and mirrors would become smaller and complicated, and then would become more difficult to be machined and measured. In this study, multi-axis controlled ultra precision machining/grinding/polishing and on-machine measurement technologies are developed for manufacturing of the complicated and micro molds. In this report, our developed grinding method of the complicated mold, ultrasonic vibration method and contact type of multi axis controlled on-machine measuring system are discussed.

Key Words: ceramic mold, ultraprecision grinding, ultrasonic vibration assisted polishing, on-measuring measurement

1. Introduction

Demands are increasing for installing of micro aspheric glass lenses to various digital devices, such as blue laser DVD pick-up systems, digital cameras and optical transmission devices in order to improve the optical performance. The micro aspheric glass lenses are generally press-molded using micro aspheric ceramic molds made of sintered tungsten carbides or silicon carbides. These ultra-precision molds and dies are generally ground with micro diamond grinding wheels that are controlled in the positioning accuracy of 1 nm, and the ground molds and dies are further polished using loose abrasives. They are finished through the compensation process based on the measured form deviation profiles. As the optical system becomes more compact and complicated and the high accuracy is required, the multi-axis controlled ultra precision machining/grinding technologies and the on-machine measurement technologies become important.

2. Micro Fresnel grinding

Fig. 1 shows a view and a schematic diagram of developed micro Fresnel-grinding process. A disk shape of resinoid bonded diamond wheel was trued on the machine, and the wheel edge was sharpened. The wheel having a knife edge was scanned along the workpiece radial position vertically.

The Fresnel shape is expressed as follows:

$$\left. \begin{aligned} Z(Y) &= \text{mod} \{g(Y), b\} \\ G(Y) &= \frac{C_v Y^2}{1 + \sqrt{1 - (K+1) C_v^2 Y^2}} + \sum_{i=1}^n C_i Y^i \end{aligned} \right\} \quad (1)$$

Where, C_v is the radius curvature, K is the conic coefficient and b is the Fresnel depth.

2.1 Vertically controlled Fresnel grinding method and system

A view of vertically controlled fresnel grinding is shown in **Fig. 1**.

The grinding spindle was actuated in X, Y and Z axes by the linear scale feedback system of 1 nm positioning resolutions. The grinding and workpiece spindles were air bearings. The wheel was simultaneous 2-axes (Y, Z) controlled [1].

Wheel positioning (Y_{NC} , Z_{NC}) is calculated as follows:

$$\left. \begin{aligned} Y_{NC} &= Y_W - R \sin \theta \\ Z_{NC} &= Z_W - R (1 - \cos \theta) \end{aligned} \right\} \quad (2)$$

Where (Y_W , Z_W) are workpiece coordinates and R is the wheel edge radius.

The wheel rotates parallel to the direction of workpiece rotation at the grinding point. By scanning the sharp wheel edged, the axis-symmetric aspheric Fresnel workpiece could be generated¹⁾.

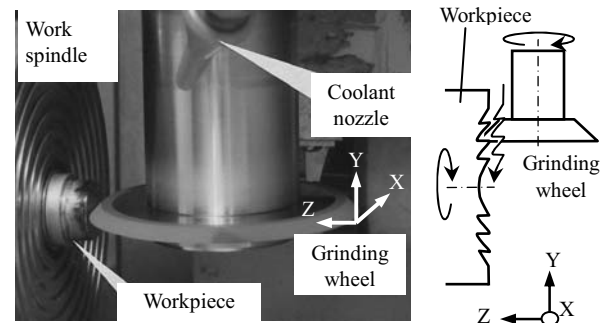


Fig. 1 Developed micro Fresnel grinding

2.2 Truing of grinding wheel by rare metal

In the conventional truing/dressing process of the resinoid bonded diamond wheel, the wheel is trued by a single crystalline diamond truer and the trued diamond wheel is dressed by a green silicon carbide (GC) stone. However, it is difficult to sharpen the wheel edge, because the GC stone is not so hard compared with the diamond wheel.

In this study, rare metals are proposed to be used as a truer/dresser of high precision and high performance. For the diamond wheel of the Fresnel lens molds, the grinding wheel is rubbed and formed for truing and dressing on the outer side surface and the bottom side surface of it, as shown in **Fig. 2**. Cylindrical diamond wheel was trued by each truer material in the conditions. Depth of cut was 1 μm and 500 times of cut was done. **Fig. 3** shows changes of truing. A truing ratio is defined by the next equation:

$$T = V_e / V_t \quad (3)$$

Where, V_e is a volume of the trued diamond wheel and V_t is a volume of the worn truer. This value, T becomes larger when the truing efficiency becomes higher.

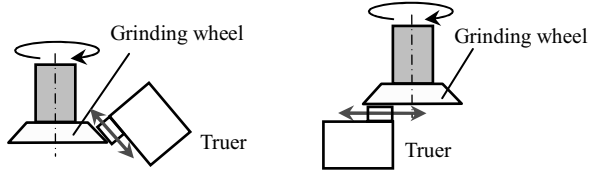


Fig.2 Proposed truing and dressing process of the resinoid bonded diamond wheel for the grinding of the Fresnel lens mold.

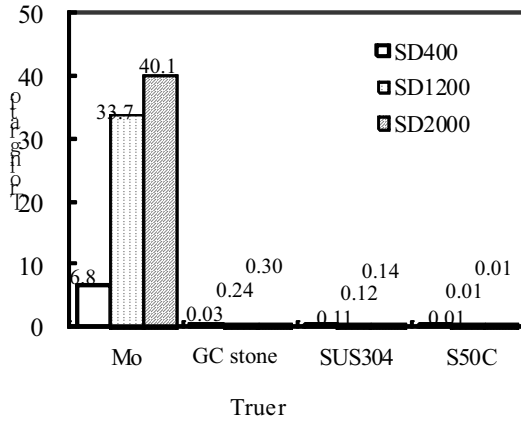


Fig. 3 Truing ratio

2.3 Grinding results

As a mold material, glassy carbon was used for high temperature glass molding. The grinding conditions are shown in **Table 1**. As a wheel, a resinoid bonded diamond wheel of #1200 in a grain size was used and was trued to be sharp edge on the machine. **Fig. 4(a)** and **(b)** show views of the glassy carbon mold ground for the diffractive optical elements (DOE). **Fig. 5** shows a form deviation profile measured by Form Talysurf. Very sharp edges were generated and a form Form accuracy of 0.1 μm P-V was obtained.

Table 1 Grinding conditions

Grinding wheel	Resinoid bonded diamond
Grain size	SD1200
Rotational rate	25,000 min^{-1}
Workpiece	Glassy carbon
Rotational rate	150 min^{-1}
Depth of cut	0.5 μm
Feed	0.3 mm/min
Coolant	Solution type

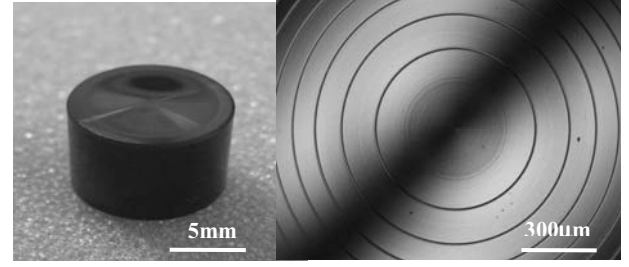


Fig.4 Ground mold for diffractive optical elements (DOE)

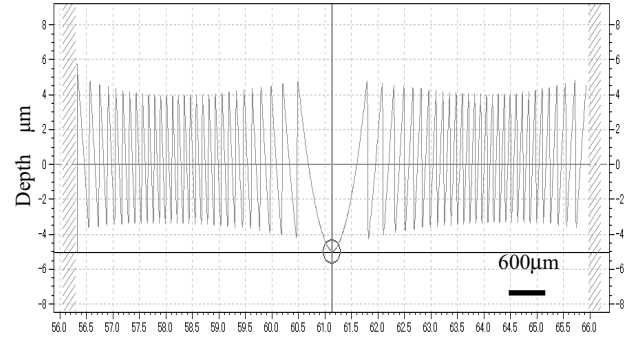


Fig.5 Measured profile of ground DOE (Reference: base aspheric)

3. Micro lens array grinding

3.1 Four-axes controlled grinding method

In micro lens array grinding, the grinding wheel moves synchronously in the same direction and at the same speed as the workpiece rotates, maintaining a constant distance between the workpiece rotation center to the machining point as shown in **Fig. 6**. The workpiece rotates 180 degrees, yielding a precision concave sphere. The lens array is produced by repeating this [2].

In four-axis controlled grinding (**Fig. 7**), the coordinates of the lens center (X_{oij} , Y_{oij}) are positioned based on the turning radius r_{ij} on the workpiece axis and rotation angle C_{oij} are expressed as follows:

$$\left. \begin{aligned} r_{ij} &= \sqrt{X_{oij}^2 + Y_{oij}^2} \\ C_{oij} &= \tan^{-1}(Y_{oij} / X_{oij}) \end{aligned} \right\} \quad (4)$$

After workpiece rotation of the angle $C_{\theta ij}$, the coordinates, arbitrary lens center ($X_{\theta ij}$, $Y_{\theta ij}$), are expressed as follows:

$$\left. \begin{aligned} X_{\theta ij} &= r_{ij} \cdot \cos(C_{oij} - C_{\theta}) \\ Y_{\theta ij} &= r_{ij} \cdot \sin(C_{oij} - C_{\theta}) \end{aligned} \right\} \quad (5)$$

The grinding wheel is moved by simultaneous 4-axis (X, Y, Z, C) with a cut in Z direction to meet Eqs. (4), (5).

3.2 Grinding results

A micro lens array mold was ground having 15 concave 1.1 mm radius spheres, spaced zigzag at 700 horizontally and vertically.

Grinding conditions are shown **Table 2**. **Fig. 8** shows a Nomarski micrograph of ground mold made of glassy carbon. **Fig. 9** shows a change of the form accuracy of all 15 lenses and the form accuracy of less than $0.2 \mu\text{mP-V}$ was obtained.

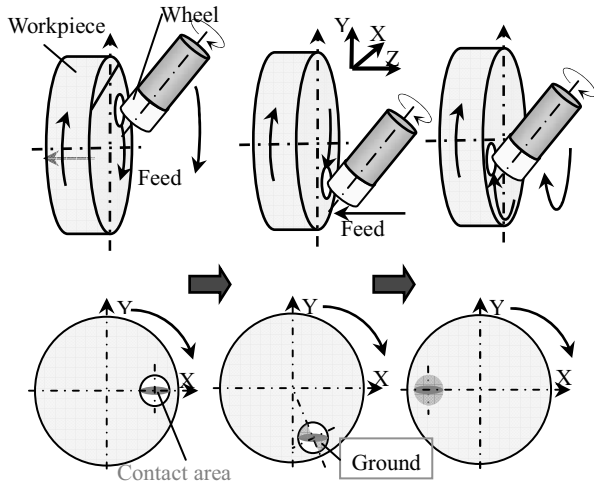


Fig.6 Micro lens array grinding

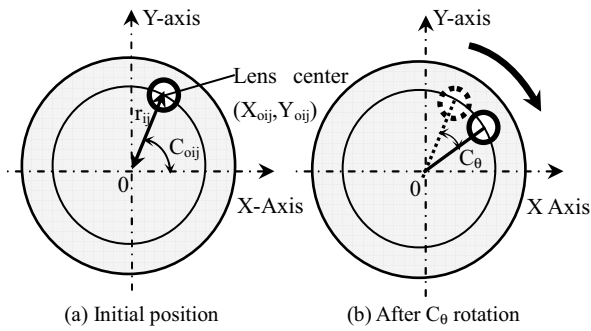


Fig.7 Tool path calculation

Table 2 Grinding conditions

Grinding machine	4-axis controlled machine
Wheel	Resinoid bonded diamond
Grain size	# 1200
Diameter	$\Phi 0.8\text{mm}$
Tip radius	$r = 0 \text{ mm}$
Rotational rate	$60,000 \text{ min}^{-1}$
Workpiece	Glassy carbon
Rotational rate	720 degrees/min
Depth of cut	$5 \mu\text{m}$
Feed rate	$0.8 \mu\text{m/min}$

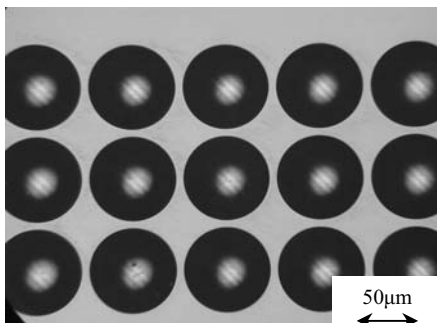


Fig.8 A micrograph of ground mold made of tungsten carbide

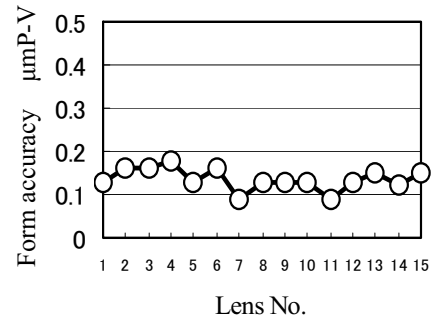


Fig.9 Changes of form accuracy

4. Precision cutting of ceramic molds by micro PCD milling tool

In order to machine micro aspheric molds and dies made of ceramics, micro milling tools made of polycrystalline diamond (PCD) are developed. In this cutting method, the materials are removed by interrupted cutting and the tool wear can be reduced. It is therefore expected that the hard ceramic can be cut with micro milling tool [3].

4.1 The PCD micro milling tool

Fig. 10 shows a PCD micro milling tool machined and the specifications are shown in **Table 3**. The tools outer diameter is $\Phi 1\text{mm}$ and 40 cutting edges are ground on the tool edge. The PCD micro milling tool was fabricated as shown in **Fig. 11**. At first the PCD wafer was bonded to a cemented carbide substrate and the bonded PCD plate was cut by wire EDM. The PCD chip was bonded on to a cemented carbide shank. Finally, the end face and side face of the PCD chip was ground and polished with a diamond wheel, and the cutting edges were ground and polished with a sharp diamond wheel.

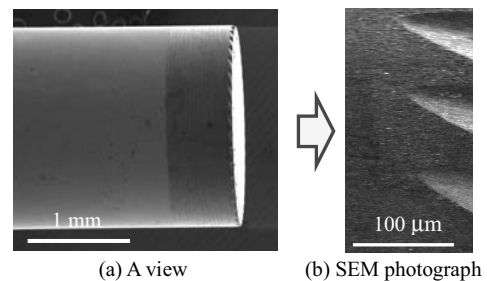


Fig. 10 Photographs of PCD micro milling tool

Table 3 Specifications of milling tool

Tool mal	Polycrystalline diamond
Particle size	$0.5 \mu\text{m}$
Diameter of cutting edge	$\Phi 2 \text{ mm}$
Tip radius	$0, 50, 100 \mu\text{m}$
Rake angle	-20 deg.
Number of cutter	40

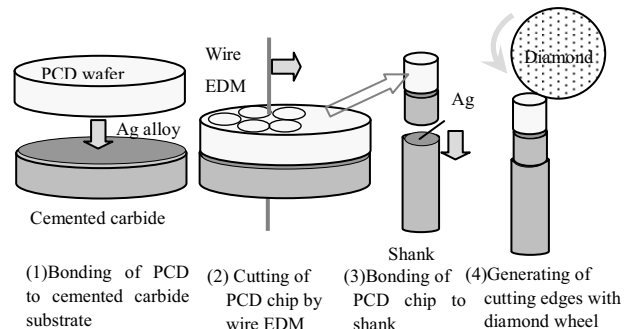


Fig. 11 Machining process of PCD micro milling tool

Fig. 12 shows a photograph and a Nomarski micrograph of machined micro array mold made of tungsten carbide. Fig. 10 shows a change of the workpiece surface roughness in machining the micro array mold. Tools with tool tip radius, $r=0\text{mm}$ was used. The surface roughness profiles were measured with non-contact surface profiler, New View 6200. In machining 2400 molds of the tungsten carbide, very smooth surface roughness of less than 10 nm Rz was obtained.

Fig. 13 shows a tool wear changes of the PCD tool in machining the micro array mold made of tungsten carbide. Tools with 3 kinds of tool tip radius, r were used. The tool tip radius became smaller, the tool wear was reduced. In the case of using the tool with tool tip radius $r=0.1\text{ mm}$, tool wear was $10\text{ }\mu\text{m}$. From the experiments, the tool wear of the PCD milling tool was 1/10th smaller than that of the resinoid bonded diamond wheel.

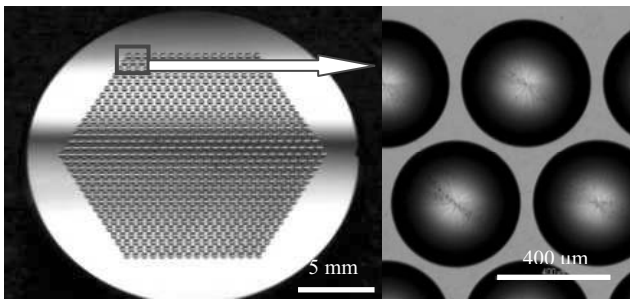


Fig.12 Photographs of machined micro array mold

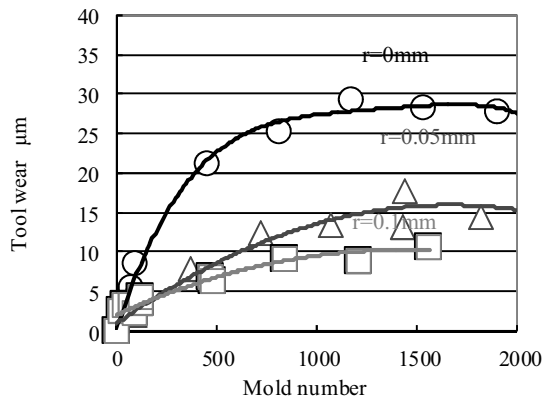


Fig. 13 Tool wear of PCD tool in machining the micro array mold

5. Micro aspheric polishing with ultrasonic two-axis vibration

Improvement aspheric molds and increasing high numerical aperture (NA) or optics with steep angle, ultrasonic two-axes vibration assisted polishing system with piezo-electric actuators and 4-axes (X,Y,Z,B) controlled was proposed and developed in order to apply to the finishing of the steep molds³⁾.

5.1 Four-axis controlled polishing machine with ultrasonic two axes vibration system

Fig. 14 shows a developed ultrasonic two axes vibration assisted polishing system. The polishing head, attached to the polisher arm, was mounted on the X-Y-Z tables. The tool local scanning speeds

were calculated based on the aspherical form and tool shape, and the NC program was generated by the PC. The B-axis tilting table could be rotated from 10 to 100 degrees in order to control polishing angle of the surface. **Fig. 15** shows a structure of the developed two-axis controlled vibrator. The disk-shape actuators generate axial vibration and the half disk-shape actuators with anti-polarity generate flexural vibration. This composite vibration is expected to improve workpiece surface roughness [4].

5.2 Polishing results

The tungsten carbide mold was tested under the conditions of **Table 4**. The aspherical workpiece was polished with the developed ultrasonic two-axis vibration polishing machine. **Fig.16** shows Nomarski micrographs of the removal function, and (a) is that by the conventional vibration and (b) is that by the proposed vibration. A surface roughness was improved to 7 nmRz by the ultrasonic two-axis vibration as shown in **Fig.17**.

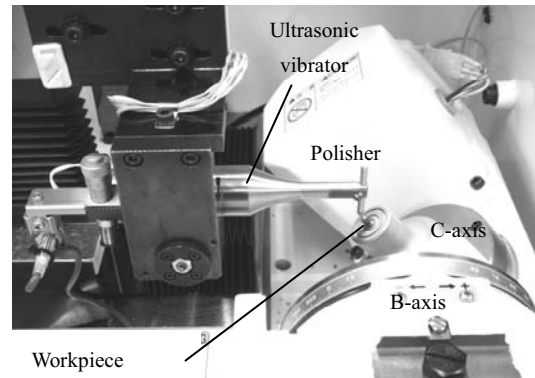
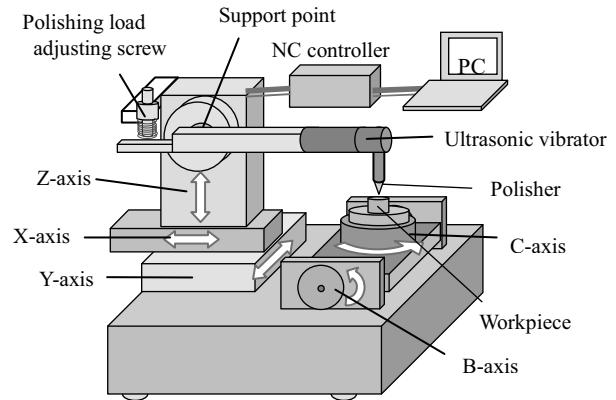


Fig. 14 4-axes controlled polishing machine with ultrasonic two axis vibration system

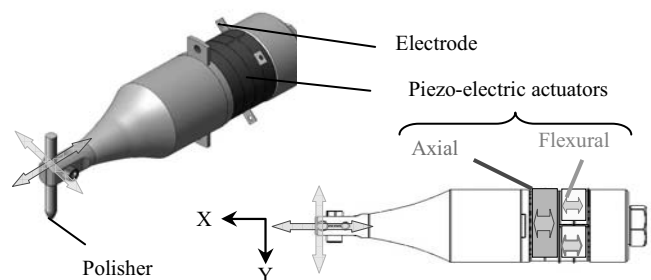
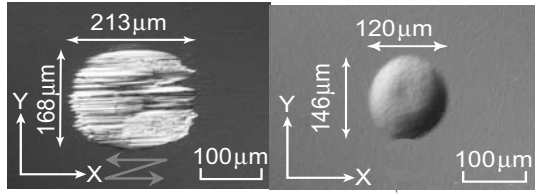


Fig. 15 Two-axis controlled ultrasonic vibrator with piezo-electric actuators

Table 4 Polishing conditions

Workpiece	Tungsten carbide
Polisher	Polyurethane
Tip radius	1.0 mm
Abrasive	Diamond slurry
Grain size	0.5 μm
Load	20 mN
Vibrator	Piezoelectric
Axial vibration	Frequency: 26.5 kHz Applied voltage: 100 V
Flexural vibration	Frequency: 21.8 kHz Applied voltage: 200 V



(a) 1 axis vibration (b) Two-axis vibration
Fig. 16 removal functions

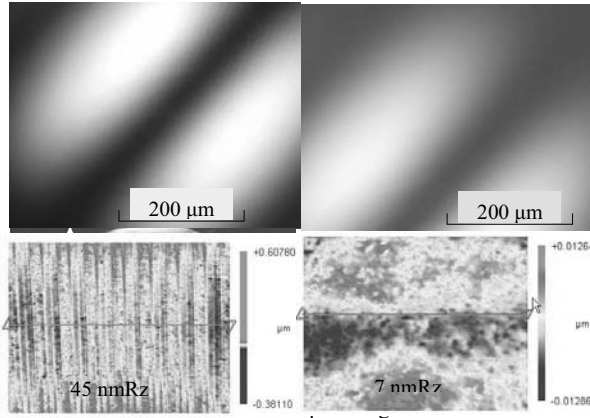


Fig. 17 Nomarski micrographs and surface roughness profiles of polished surface

6. Multi-axis controlled on-machine measurement system

The 45 degrees tilted multi-axis controlled on-machine measurement system was developed to measure aspheric optical parts with steep surface angles for large numerical aperture (NA)⁴⁾.

6.1 45degrees tilted and new scanning method

In order to reduce the measurement errors caused by the probe deformation, a new probe scanning method is proposed. The probe is tilted at 45 degrees from the workpiece axis on the X-Z plane and the probe scans 3-dimensionally so as to keep the contact angle between the probe axis and the contact surface constant in order to reduce the change in the friction force between the measuring probe and measured workpiece as shown in **Fig. 18**, while the probe scans conventionally in 2 dimensions on the Y-Z plane.

6.2 Probe path calculation

The positional relationship between the ball probe and workpiece is shown in **Fig. 18(b)**. The normal vector \mathbf{n} at the contact point between

the probe and workpiece surface is given by:

$$\mathbf{n}(a,b,c) = \left(-\frac{\partial f}{\partial X}, -\frac{\partial f}{\partial Y}, 1 \right) \quad (6)$$

The vector \mathbf{CO} between the probe center O and the contact point C is given by:

$$\mathbf{CO} = \left(\frac{a}{l}r, \frac{b}{l}r, \frac{c}{l}r \right) \quad (7)$$

Where, $l = (a^2 + b^2 + c^2)^{0.5}$, and r_p is the ball probe radius respectively. When the probe is tilted at 45 degrees from the Y-Z plane, the directional vector of the probe \mathbf{p} is given by $\mathbf{p} = (1, 0, 1)$. From Equations (6) and (7), the following relation is obtained:

$$b^2 = 2ac \quad (8)$$

The contact point coordinate $C(X_c, Y_c, Z_c)$ is expressed as follows:

$$\left. \begin{aligned} X_c &= R \sin \tau \\ Y_c &= R \cos \tau \\ Z &= f(R) \end{aligned} \right\} \quad (9)$$

Where, R is the workpiece radial position of and τ is angle of the C from Y axis.

From the Equations (6) and (9), the following relationship is obtained:

$$\mathbf{n}(a,b,c) = (-f'(R) \cos \tau, f'(R) \sin \tau, 1) \quad (10)$$

From Equations (7) and (9), the angle τ is given by:

$$\sin \tau = \frac{l}{f'(R)} + \sqrt{\frac{l}{f'(R)} + 1} \quad ; \text{ for convex shape} \quad (11.1)$$

$$\sin \tau = \frac{l}{f'(R)} - \sqrt{\frac{l}{f'(R)} + 1} \quad ; \text{ for concave shape} \quad (11.2)$$

In order to determine the probe scanning path, first, the angle τ is calculated at the radius position R as shown above, then the contact point coordinate on the workpiece surface $C(X_c, Y_c, Z_c)$ is calculated yielding ball probe center coordinate $O(X_o, Y_o, Z_o)$. The probe scans the workpiece surface 3-dimensionally in the proposed method, while it scans 2-dimensionally in the X-Z plane in the conventional method.

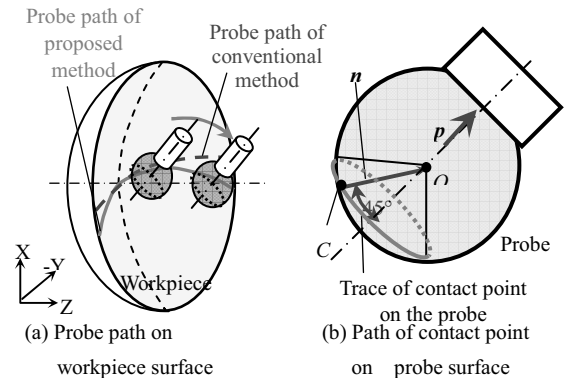


Fig. 18 Principle of 45 degrees tilted scanning principle

5.3 45degrees tilted and new scanning method

Fig. 19 shows a schematic diagram of the developed air slider and the measurement unit made of SIALON ceramics. The density is 1/2.5 and the thermal expansion coefficient of SIALON is 1/10 as compared to steel. The air slider is supported by an air gap of 2 μm on both sides of the air bearings. In the center of the slider, there is a gap of about 100 μm . The air is supplied through this port and released through one side of the port while there is no release port at the other side. The pushing force and the pulling force are generated by adjusting the air pressure in both sides. Low contact force of 0.1 mN can be obtained by this mechanism. A small glass linear scale is attached to the rear end of the slider. The amount of its movement is measured with the detector of the linear glass scale in 0.14 nm resolution [5].

Fig. 20 shows the form deviation profiles measured by the proposed measurement method compared with the conventional one. In case of the conventional one, the measurement error increases as a sweep angle increases up to 50 degrees because of the contact force angle change of the probe. On the other hand, in case of the proposed method, the form deviation profile is measured correctly.

7. Summary

Demands of micro aspheric optical components such as lenses and mirrors are increasing and the molds shapes of lens and mirrors would become smaller and complicated. In this study, multi-axis controlled ultra-precision machining, grinding, polishing and on-machine measurement technologies are developed for manufacturing of the complicated and micro molds. In this report, our developed grinding method of the complicated mold, ultrasonic vibration method and contact type of multi axis controlled on-machine measuring system were discussed.

References

- [1] Y. Yamamoto, H. Suzuki, T. Moriwaki, T. Okino and T. Higuchi: Precision Grinding of Micro Fresnel Lens Molding Die (2nd report), Journal of Japan Society for Precision Engineering, 73(6), pp. 688-692 (2007) [in Japanese].
- [2] Y. Yamamoto, H. Suzuki, T. Onishi, T. Okino and T. Moriwaki: Precision Grinding of Microarray Lens Molding Die with 4-axes, Science and Technology of Advanced Materials, 8, pp. 173-176 (2007).
- [3] Suzuki H., Moriwaki T., Yamamoto Y., Goto Y., 2007, Precision Cutting of Aspherical Ceramic Molds with Micro PCD Milling Tool, Annals of the CIRP, 56/1: 131-134.
- [4] H. Suzuki, T. Moriwaki, T. Okino, Y. Ando: Development of Ultrasonic Vibration Assisted Polishing Machine for Micro Aspheric Die and Mold, Annals of the CIRP, 55(1), pp. 385-388 (2006).
- [5] H. Suzuki, T. Onishi, T. Moriwaki (1), M. Fukuta, J. Sugawara: Development of 45 degrees tilted on-machine measuring system for small optical parts, Annals of the CIRP, 57(1), M10 (2008).

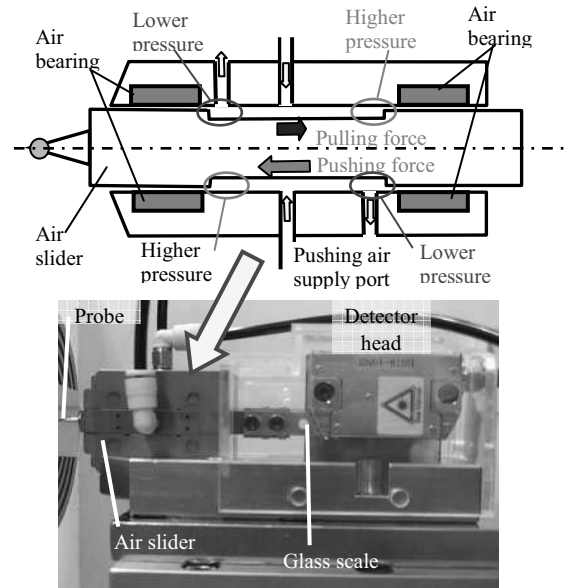
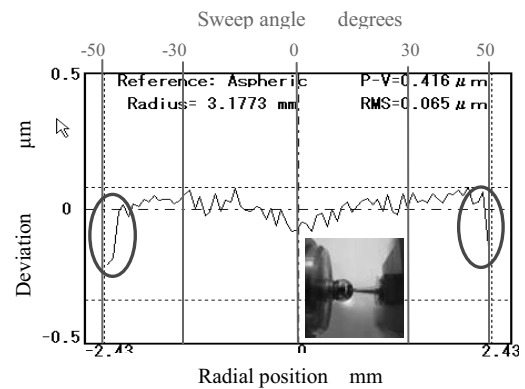
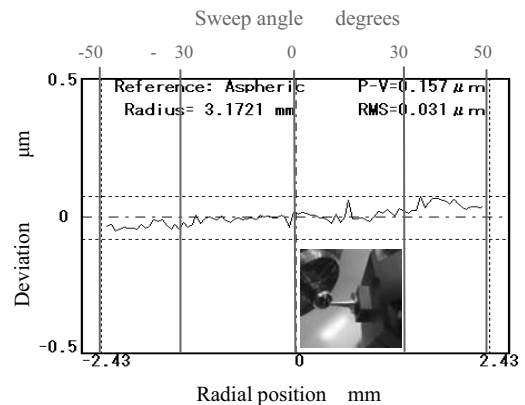


Fig. 19 Schematic diagram and view of developed air slider for measurement unit



(a) Conventional scanning method



(b) Proposed 45 degrees tilted method

Fig. 20 Measured form deviation profiles.